JOURNAL OF MATERIALS SCIENCE 16 (1981) 151–158

Nickel sulphide inclusions in glass: an example of microcracking induced by a volumetric expanding phase change

M. V. SWAIN*
Saint Gobain Recherche, Aubervilliers, France

Microcracking about inclusions of nickel sulphide in soda-lime glass has been studied. These cracks are nucleated by the volumetric expansion that accompanies the α–β phase transformation in nickel sulphide. The α-phase is metastable and, upon transformation to the β-phase, is accompanied by a volumetric expansion of about 4%. A simple generalized fracture mechanical analysis of the cracking about such inclusions is developed. Firstly, crack initiation about an inclusion is considered; this is then extended to consider inclusions within a thermally tempered plate. The critical dimensions of the inclusion to initiate microcracking in an annealed specimen and to cause spontaneous fracture of a tempered plate are predicted. Observations of nickel sulphide inclusions in annealed and tempered specimens support the predictions. The implications of this work with regard to the addition of fine dispersions of zirconia to ceramics are pointed out.

1. Introduction

The presence of nickel sulphide (NiS) inclusions in soda-lime glass becomes a serious problem when the glass is thermally tempered. These inclusions, which are generally spherical or slightly elliptical although occasionally cigar shaped inclusions are found, undergo a volume expanding phase change upon cooling. This volumetric expansion is sufficient to nucleate microcracks which, in tempered glass, propagate in the internal tensile stress field, resulting in the destruction of the body. This phenomenon was first appreciated by Ballantyne [1] who correctly identified the inclusions and found that the position of the inclusion within the plate was important. More recently Hsioa [2] has presented further fractographic evidence to support the conclusions of Ballantyne.

The complete Ni–S phase diagram is very complex, see Wagner [3] for a recent review, but it has been found [4] that NiS inclusions with the approximate composition 65 wt% Ni–34 wt% S, commonly called millerite, are primarily responsible for the spontaneous fracture of tempered glass. Millerite undergoes a phase transformation from the high temperature, hexagonal α-phase to the low temperature, rhombohedral β-phase at a temperature of 380° C. The precise temperature of the phase change is strongly dependent upon stoichiometry. It has been found that in quickly-cooled glass only the α-phase is present in the inclusion. However, upon subsequent heating the inclusion may transform to the β-phase, the time taken for the transformation being a sensitive function of temperature.

The aim of the present study has been to observe microcracks about phase transformed inclusions in glass and to compare these observations with a simple fracture mechanical analysis of the problem. Previous studies of the energetics of cracking about inclusions with thermal expansion coefficients different from the matrix have been made by Davidge and Green [5], and Lange [6]. Evans [7] has also carried out a fracture mechanical analysis of this problem incorporating the influence of an applied tensile stress. The present treatment differs slightly from that of Evans by drawing a strong analogy with current developments in indentation fracture mechanics [8, 9].

---

*Present address: CSIRO, Division of Materials Science, P.O. Box 4331, Melbourne, 3001 Victoria, Australia.

TABLE I Mechanical and thermal properties of NiS and glass

Property	Glass	NiS	
		α	β
Young's modulus, E (N m^{-2})	7.0×10^{10}	8.0×10^{10}	7.0×10^{10}
Poisson's ratio, ν	0.23	0.27	0.20
Density, ρ (Kg m^{-3})	2.51×10^3	5.46×10^3	5.25×10^3
Thermal expansion coefficient, α ($^\circ\text{C}^{-1}$)	88×10^{-7}	163×10^{-7}	145×10^{-7}

The latter approach enables a simple extension of the analysis to include the presence of tensile tempering stresses.

2. Theoretical considerations

The volumetric expansion, $\Delta V/V$, of a particle which undergoes an isotropic phase transformation is given by

$$\frac{\Delta V}{V} = \frac{\rho_\alpha}{\rho_\beta} - 1, \tag{1}$$

where ρ_α and ρ_β are the densities of the α- and β-phases, respectively. Using the values listed in Table I, this corresponds to a volumetric expansion of 4%, which is in good agreement with the expansion proposed by Hsiao [2].

The stresses developed about a spherical isotropic inclusion in a material, with the co-ordinate system of Fig. 1, are given by

$$\sigma_r = -2\sigma_t = -P_0\left(\frac{R}{r}\right)^3 ; r \geqslant R, \tag{2}$$

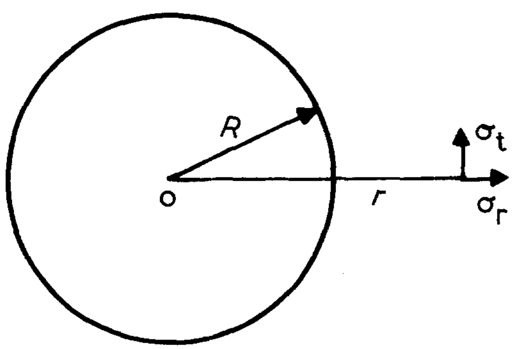

Figure 1 The co-ordinate system and mechanical stresses about an inclusion.

where σ_r is the radial stress, σ_t the circumferential or "hoop" stress and r is the distance from the centre of the inclusion, and within the inclusion

$$\sigma_r = \sigma_t = -P_0 ; 0 \leqslant r \leqslant R, \tag{3}$$

where P_0 is the hydrostatic pressure and R is the radius of the inclusion.

The resulting radial strain $\Delta R/R$ may be shown to be given by [10]

$$\frac{\Delta R}{R} = P_0\left(\frac{1+\nu_1}{2E_1} + \frac{1-2\nu_2}{E_2}\right) = \frac{\Delta V}{3V}, \tag{4}$$

where ν_1 and E_1 and ν_2 and E_2 are the Poisson's ratio and Young's modulus of the host material and the inclusion, respectively.

The resulting hydrostatic pressure on substitution for $\Delta V/V$ is

$$P_0 = -\left(\frac{\rho_\alpha}{\rho_\beta} - 1\right) \Big/ \left(\frac{1+\nu_1}{2E_1} + \frac{1-2\nu_2}{E_2}\right). \tag{5}$$

The hydrostatic pressure resulting from the α–β phase transformation of NiS in soda-lime glass, using the values listed in Table I[*], is 834 MPa. In addition, there will be stresses resulting from differences in thermal expansion coefficient and mismatch of elastic constants. As the difference in the latter is small, see Table I, this factor will be neglected. The stresses resulting from the differences in thermal expansion coefficients are given by [11]

$$\sigma_r = 2\sigma_t = \frac{(\alpha_{\text{glass}} - \alpha_{\text{NiS}})(T_g - T)}{\left(\frac{1+\nu_1}{2E_1} + \frac{1-2\nu_2}{E_2}\right)}\left(\frac{R}{r}\right)^3 = P_{\text{OT}}\left(\frac{R}{r}\right)^3 \tag{6}$$

where T_g and T are the softening temperature of glass (~ 550° C) and the temperature under consideration and α_{glass} and α_{NiS} are the thermal expansion coefficients of the glass and nickel sulphide. The resulting value of P_{OT}, using a mean value of α_α and α_β for α_{NiS}, is -219 MPa. Thus, the resulting hydrostatic pressure within the phase transformed sphere is 615 MPa.

An exact expression for the stress intensity factor is somewhat difficult to determine. This is because, initially, the crack nucleates at a localized position and grows before encircling the inclusion

---

[*] In all cases the value of E_2 has been taken as the mean of E_α and E_β.

and further extending. Evans [7] has offered a solution to this problem but has stressed its limited application. In this work, an alternative approach is developed which has its origins in the analysis of cracks about indentations. In both cases cracks are developing in spatially varying stress fields. Considering the initiation phase, an approach adopted by Lawn and Evans [8] for the initiation of cracks beneath a pointed indenter is followed. These authors used a model involving a simple linear approximation to the stress field which was applied only until a certain distance, b, from the initiation site; thereafter the stress was set as zero:

$$\sigma_t = \sigma_m\,(1-x/b);\; x \leqslant b \qquad (7)$$

$$\sigma t = 0 \qquad ;x \geqslant b, \qquad (8)$$

where b is a constant, which in the present case is related to the inclusion size, and $\sigma_m = P_0/2$. The stress intensity factor for an axial symmetric crack with the co-ordinate system given in Fig. 2 is then [12]

$$K = \frac{2}{(\pi c)^{1/2}} \int_0^c \frac{x\,\sigma_t(x)\,dx}{(c^2-x^2)^{1/2}}. \qquad (9)$$

Substitution from Equations 7 and 8 for $\sigma_t(x)$ into Equation 9, and integrating, gives

$$K = 2\sigma_m \left(\frac{c}{\pi}\right)^{1/2} (1-\pi c/4b);\; c \leqslant b \qquad (10)$$

$$= 2\sigma_m \left(\frac{c}{\pi}\right)^{1/2} \left[1 - \tfrac{1}{2}\,(1-b^2/c^2)^{1/2} - \tfrac{1}{2}\left(\frac{c}{b}\right);\sin^{-1}\left(\frac{b}{c}\right)\right];\; c \geqslant b. \qquad (11)$$

Substituting for σ_m and putting $b = \eta R$ in Equations 10 and 11 gives, in normalized form

$$\frac{K}{P_0\left(\frac{R}{\pi}\right)^{1/2}} = \left(\frac{c}{R}\right)^{1/2} \left[1 - \frac{\pi}{4\eta}\left(\frac{c}{R}\right)\right];\; c \leqslant \eta R \qquad (12)$$

$$\frac{K}{P_0\left(\frac{R}{\pi}\right)^{1/2}} = \left(\frac{c}{R}\right)^{1/2} \left[1 - \tfrac{1}{2}\left(1-\eta^2\frac{R^2}{c^2}\right)^{1/2} - \tfrac{1}{2}\eta\,\frac{c}{R}\sin^{-1}\left(\frac{\eta R}{c}\right)\right];\; c \geqslant \eta R. \qquad (13)$$

On plotting the normalized stress intensity factor as a function of normalized crack length, see Fig. 3,

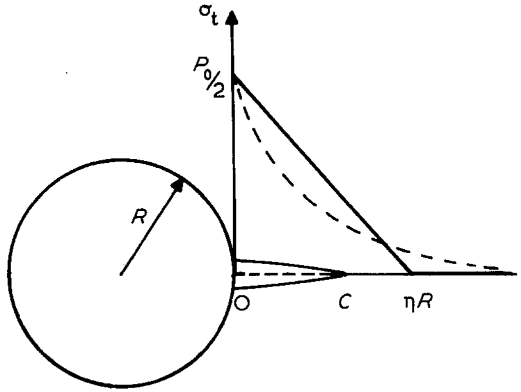

Figure 2 The co-ordinate system used to calculate the stress intensity factor for initial crack extension about an inclusion. Also included is a schematic diagram of the stress and linear approximation of the stress.

it can be seen that the curve is a sensitive function of η.

Once the crack has been initiated it generally encircles the inclusion and the above expression is no longer valid. Instead, again using an indentation fracture mechanical analogy, the crack is considered to be driven by an equivalent point force.

Following Lawn and Fuller [9], the resolved force resulting from the hydrostatic pressure of the particle in the direction normal to the crack plane and at the middle of the inclusion is considered. The resulting stress intensity factor is [12]

$$K = \frac{P_e}{(\pi c')^{3/2}} = \frac{2P_0\,\pi R^2}{3\,(\pi c')^{3/2}}, \qquad (14)$$

where P_e is the equivalent point load, c' is the crack length with the origin at the centre of the inclusion and $\frac{2}{3}P_0$ is the averaged normal pressure

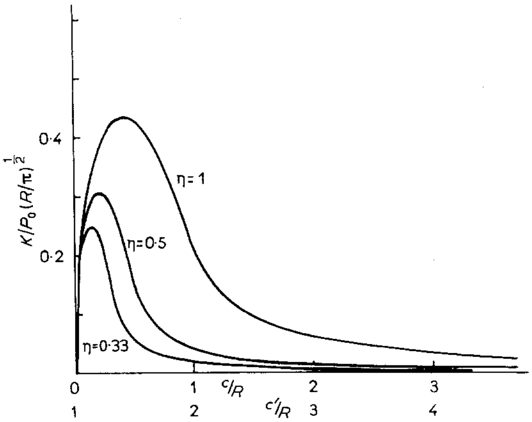

Figure 3 A plot of normalized stress intensity factor against normalized crack length for three values of η.

over the diameter of the inclusion. Again, normalizing gives

$$\frac{K}{P_0\left(\frac{R}{\pi}\right)^{1/2}} = \frac{2}{3\left(\frac{c'}{R}\right)^{3/2}} \tag{15}$$

This functional dependence is strictly valid only when $c' \gg R$.

In utilizing the last expression, it has been implicitly assumed that uncoupling of the inclusion–glass interface occurs. Otherwise, the opening of the crack adjacent to the inclusion would be limited due to the radial stresses about the inclusion. Some justification for this assumption comes from the observations that, generally, the inclusion is only in one of the two fragments of glass after spontaneous fracture of the tempered glass.

When the glass is thermally tempered, a parabolic stress distribution results within the plate, the maximum tensile stress in the middle being half the surface compressive stress. The stress intensity factor for a crack at the centre of the plate, of radius c′, is

$$K = 2\sigma_0 \left(\frac{c'}{\pi}\right)^{1/2}, \tag{16}$$

where σ_0 is the maximum tensile stress. The influence of the position of the inclusion may be readily included in the analysis, if it is assumed that the stress in the vicinity of the particle and crack is constant and is given by

$$\sigma_y = \sigma_0\,(1 - 3y^2/d^2), \tag{17}$$

where y is the distance from the centre of the plate, and $2d$ is the plate thickness. Combining Equations 16 and 17 and normalizing gives

$$\frac{K}{P_0\left(\frac{R}{\pi}\right)^{1/2}} = \frac{2\sigma_0}{P_0}\left(\frac{c'}{R}\right)^{1/2}\left(1 - \frac{3y^2}{d^2}\right). \tag{18}$$

A plot of this expression for various values of σ_0/P_0 is shown in Fig. 4, for $y = 0$. Also shown in Fig. 4 is Equation 15 and the summation of these two expressions for different values of σ_0/P_0. The loci of the minima of the normalized stress intensity factor, for different values of σ_0/P_0, may readily be found by differentiating the sum of Equations 15 and 18, and is plotted in Fig. 5. The critical radius of an inclusion with internal pressure P_0 in a tensile stress of σ_0 for spontaneous fracture is then

$$R = \frac{\pi K_{\text{Ic}}^2}{7.1 P_0^2 (\sigma_0/P_0)^{3/2}}. \tag{19}$$

This expression should also be applicable to annealed plates or bottles containing inclusions under tension [13].

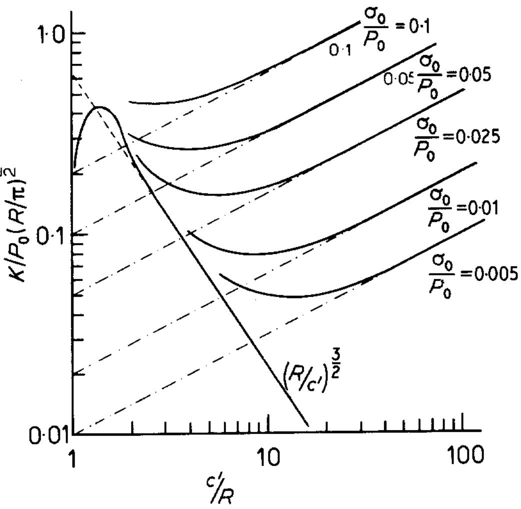

Figure 4 A plot of normalized stress intensity factor against normalized crack length according to Equations 15 and 18. The co-ordinate system is that given in Fig. 1.

3. Experimental results

A number of well-annealed soda-lime glass plates containing a small percentage of nickel (< 0.6 wt%)

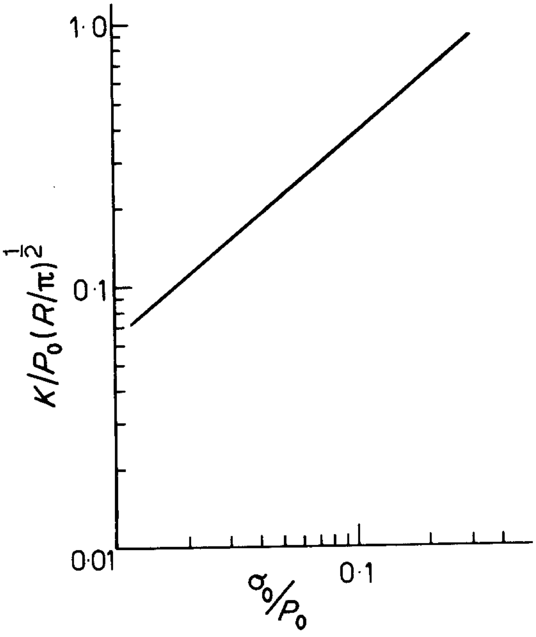

Figure 5 The loci of the minima of the normalized stress intensity factor as a function of normalized tempering stress.

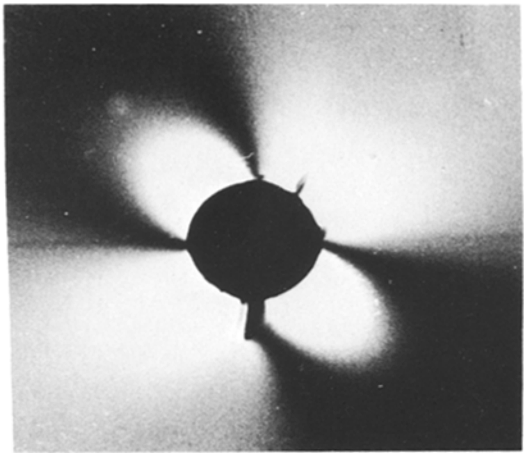

Figure 6 A phase transformed inclusion viewed in transmitted polarized light.

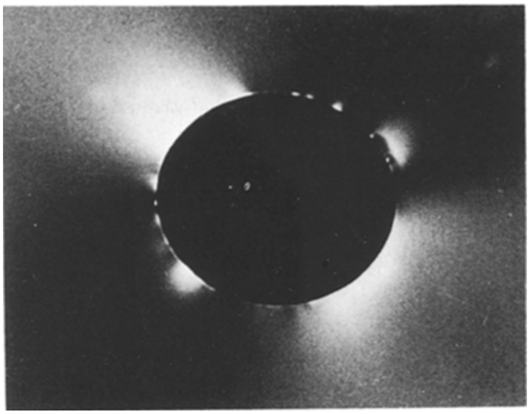

Figure 8 Observation of the inhomogeneities about a phase transformed particle viewed in transmitted polarized light.

were carefully examined for NiS inclusions. The particles which had undergone a phase transformation were readily detected using transmitted polarized light. A typical observation of such an inclusion is shown in Fig. 6. The dimensions of the inclusion and any associated cracks were measured. The results of some 50 observations are shown in Fig. 7.

Cracks were not observed around particles of less than 60 µm in diameter. The length of the cracks was found to increase with inclusion size. Sometimes no cracks were observed around the inclusion, despite the presence of a significant strain field. In other cases the strain field about the particle was relatively weak and again no cracks were observed. On closer examination of the strain field around an inclusion there were a number of inhomogeneities with localized higher strains as shown in Fig. 8. These inhomogeneities presumably provided the nucleation sites for crack formation.

In addition, two attempts were made to temper small samples of the glass containing the NiS inclusions. In one case, the glass spontaneously ruptured shortly after it was removed from the furnace. In the other sample, which had been less strongly tempered, there was evidence of crack extension around an inclusion. In the latter sample, it was found that many particles which had previously shown high strain fields and associated cracks now showed no such effect. This most probably occurred because of the reversibility of the α–β phase transformation. Closer inspection of the sample that spontaneously fractured re-

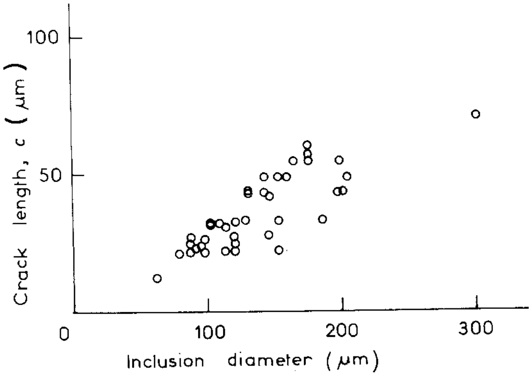

Figure 7 Crack lengths about phase transformed particles of varying diameters.

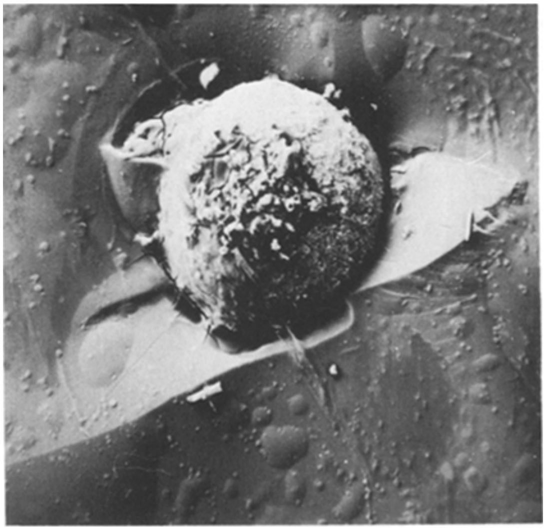

Figure 9 A NiS inclusion at the origin of a spontaneously fractured tempered plate; inclusion diameter 186 µm.

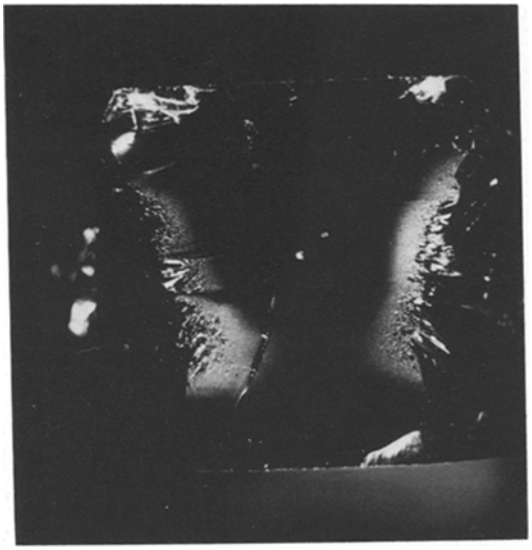

Figure 10 NiS inclusion and surrounding fracture mirror; plate width 11 mm.

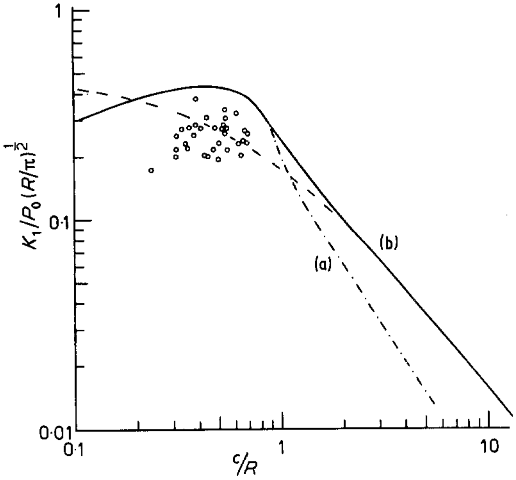

Figure 11 A re-plot of the observations in Fig. 8 in normalized parameters with $K_{1c} = 0.75\,\mathrm{MN\,m^{-3/2}}$ and $P_0 = 615\,\mathrm{MPa}$. Also plotted are (a) Equations 12 and 13, with $\eta = 1.0$, and (b) Equation 15. Note the log–log scale for both co-ordinates.

vealed a NiS inclusion situated near the centre of the plate to be responsible fo the fracture, see Fig. 9. Surrounding the inclusion was a fracture mirror, Fig. 10. In the other specimen, with the inclusion near the centre of the plate the crack had more than doubled its length in the weak tensile stress field (10 MPa) induced by the tempering.

Observations of tempered plates with NiS inclusions that had spontaneously fractured revealed [14] that fracture generally initiated from particles greater than 110 μm in diameter located in the tensile stress field near the middle of the plate. Inclusions of diameter in the range 80 to 110 μm were sometimes responsible for spontaneous fracture, whereas those inclusions of diameter less than 80 μm were not dangerous. The tensile stress in these plates was in the range 50 to 60 MPa. When plate fracture did occur from inclusions closer to the edge of the plate it was invariably initiated from particles much larger than the minimum size.

4. Discussion

The observations, shown in Fig. 7, of cracks around transformed particles have been replotted in normalized units in Fig. 11. Also included in Fig. 11 is the curve predicted by Equations 12 and 13 when $\mu = 1.0$. Almost all the points lie either below or on this curve. There are numerous possible reasons for this, including incomplete phase transformation, and consequent overestimation of P_0, and, as shown by Tabuchi [15], the often inhomogeneous nature of these inclusions, see Fig. 8. It is now possible to determine the minimum size of a NiS inclusion that is capable of crack initiation. The maximum value from the curve in Fig. 3 with $\eta = 1.0$ is about 0.44*. Then, from Equation 12,

$$R \geqslant \frac{\pi K_{1c}^2}{(0.44 P_0)^2}, \tag{20}$$

that is, $R \geqslant 24.1\,\mu\mathrm{m}$ with $K_{1c} = 7.5 \times 10^5\,\mathrm{N\,m^{-3/2}}$, and $P_0 = 615\,\mathrm{MPa}$.

This value is in reasonable agreement with a minimum value of 32 μm for the smallest radius of an inclusion with an associated crack. This agreement is hardly surprising considering the somewhat experimental manner in which η was determined. By way of comparison, Lange [16] has recently proposed a critical condition for crack extension based on the analysis of Evans [7]. The critical sphere size radius, R_c, below which crack extension does not occur is given by

$$R_c \simeq \frac{15 K_{1c}^2}{P_0^2} \tag{21}$$

---

*A somewhat better fit to the data in Fig. 11 is obtained with $\eta = 0.8$, in Equations 12 and 13, giving a maximum value of 0.4, and a critical NiS inclusion radius of 29.2 μm.

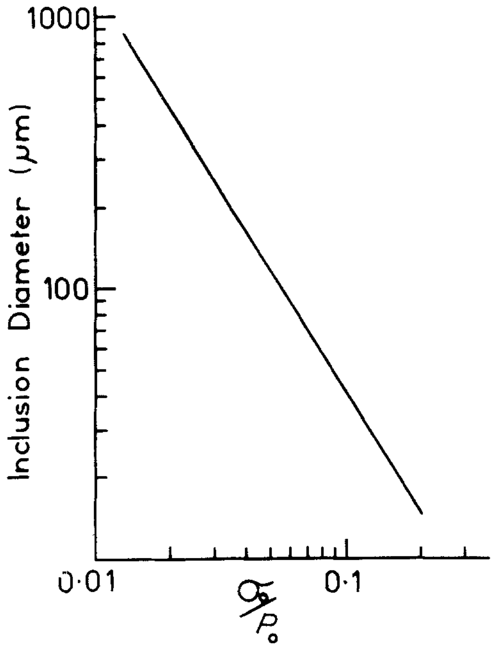

Figure 12 A plot of critical inclusion diameter as a function of the tempering level.

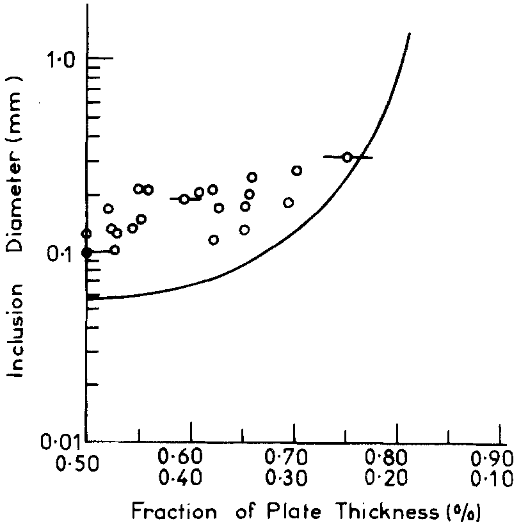

Figure 13 A plot of critical inclusion diameter with distance from the centre of the plate with a maximum internal tension of 50 MN m^{-2}. Data points obtained from [1]. Bars indicate the inclusion width.

that is, $R_c \geqslant 22.3\,\mu\text{m}$, which is in good agreement with the present analysis and observations.

The influence of the tempering or applied stress level on the normalized stress intensity factor has been given in Figs 5 and 6. From Equation 19 it is possible to determine the minimum size of an inclusion necessary to spontaneously fracture a glass plate of a specific tempering or applied stress level. The variation of the critical inclusion diameter with normalized stress level is shown in Fig. 12.

The diameter of an inclusion, predicted to cause spontaneous fracture in a tempered plate with internal tensile stress of 50 MPa, is 57 μm, which is in good agreement with observation. The effect of the position of the inclusion within the plate on the critical size of the inclusion is shown in Fig. 13 when the maximum tensile stress is 50 MPa. This curve is likely to be an overestimate of the minimum inclusion dimension for thin plates because of the stress variation across the inclusion and crack in this case. Also included in Fig. 13 are some observations by Ballantyne [1] of the dimensions and positions of NiS inclusions in tempered glass plates which had spontaneously shattered. These observations are in good agreement with prediction but do indicate that the stress gradient becomes more critical as the inclusion approaches the compressive zone.

5. Conclusions

It has been shown that fracture mechanics considerations suggest that there are two critical dimensions of nickel sulphide inclusions in glass. For annealed glass there is a critical size of inclusion above which nucleation of microcracks can take place. In tempered glass there is another critical inclusion size, which is dependent upon both the tempering stress and location of the inclusion, leading to spontaneous fracture of the body. Whilst the generalized analysis was verified for the particular case of a NiS inclusion in glass, a similar analysis should be useful for any inclusion which develops a positive hydrostatic pressure within the glass, regardless of whether this arises as a result of a phase change or a difference in thermal expansion coefficient of the inclusion and the glass.

Currently, there is considerable interest in the addition of zirconia to a number of other ceramic systems because of the enhanced toughening that may be achieved. One explanation of this toughening is the concept of microcracking ahead of a crack growing through the material [17]. This is possible because particles of zirconia transforming from the higher temperature tetragonal phase to the lower temperature monoclinic phase undergo both shear and volumetric strains. In the larger particles the shear strains are significantly reduced by twinning within the grain. Hence, a similar analysis to the one outlined in this work might be expected to predict the minimum particle size for the onset of microcracking and the zone of the microcrack extension about particles ahead of an opening macroscopic crack.

Acknowledgements

The author wishes to thank St. Gobain Industries for support, and laboratory facilities during the course of this work. Also thanks due to C. Guillemet and D. Quiquampoix for extensive discussions and availability of unpublished work and P. Sanford for comments on the manuscript.

References

1. E. R. BALLANTYNE, CSIRO, Division of Building Research, Melbourne, Australia, Report 061-5 (1961).
2. C. C. HSIAO, *Fracture* 3 (1978) 985.
3. R. WAGNER, *Glastechn. Ber.* 50 (1977) 296.
4. D. QUIQUAMPOIX, private communication, 1978.
5. R. W. DAVIDGE and J. T. GREEN, *J. Mater. Sci.* 3 (1968) 629.
6. F. F. LANGE, "Fracture Mechanics of Ceramics" Vol. 2, edited by R. C. Bradt, D. P. Hasselman and F. F. Lange (Plenum Press, New York, 1974) p. 599.
7. A. G. EVANS, *J. Mater Sci.* 9 (1974) 1145.
8. B. R. LAWN and A. G. EVANS, *ibid.* 12 (1977) 2195.
9. B. R. LAWN and E. R. FULLER, *ibid.* 10 (1975) 2016.
10. J. SELSING, *J. Amer. Ceram. Soc.* **44** (1961) 419.
11. D. WEYL, *Ber. Deut. Keram. Ges.* **36** (1959) 319.
12. G. C. SIH, "Handbook of Stress Intensity Factors" (Lehigh University Press, Lehigh, 1973).
13. M. V. SWAIN, St. Gobain Industries, Aubervilliers, France, S.C.R. report 4390/78.
14. St. Gobain Industries, Aubervilliers, France. Unpublished work.
15. H. TABUCHI, Proceedings of the International Congress on Glass, Kyoto, 1974, Vol. 3, p. 54.
16. F. F. LANGE, "Fracture of Ceramics" Vol. 4, edited by R. C. Bradt, D. P. H. Hasselman and F. F. Lange (Plenum Press, New York, 1978) p. 789.
17. N. CLAUSSEN, *J. Amer. Ceram. Soc.* 59 (1976). 49.

Received 21 December 1979 and accepted 30 June 1980.